# Altered gut microbiota and host pathways in obesity-related knee osteoarthritis

J. Huang[1], M. Liu[1], H. Zhang[2], G. Sun[2], A. Furey[3], P. Rahman[2], G. Zhai[1]

*[1]Human Genetics & Genomics, Division of BioMedical Sciences, [2]Discipline of Medicine, [3]Discipline of Orthopaedic Surgery, Faculty of Medicine, Memorial University of Newfoundland, St. John's, NL, Canada.*

## Abstract

### Objective

*To investigate gut microbial alteration and their functional consequences in obesity (OB)-related knee osteoarthritis (OA) by integrating microbiome with metabolomic, proteomic, and dietary data.*

### Methods

*Fecal and fasting plasma samples were collected from 91 knee OA patients and 12 OA-free controls, classified into four subgroups based on OB and OA status: 66 $OB^+OA^+$, 25 $OB^-OA^+$, 5 $OB^+OA^-$, and 7 $OB^-OA^-$. 16S rRNA gene sequencing was performed to profile gut microbiota. MaAsLin2 modelling was applied, and dietary intake was incorporated into the models. Plasma metabolomics (n=630 metabolites) and proteomics (n=5,416 proteins) were integrated with microbial signatures to assess functional associations.*

### Results

*$OB^+OA^+$ patients exhibited significantly lower α- and β-diversity than $OB^-OA^+$ ($p<0.05$). Seventeen microbial taxa were identified to be significantly associated with $OB^+OA^+$ (all $p<7.65\times10^{-5}$ after correcting tests for 654 ASVs), and 16 of them remained significant after adjustment for age, sex, antibiotic use, and dietary intake. PICRUSt2-based predictive analysis on these taxa suggested that bile acid biosynthesis was upregulated in $OB^+OA^+$ group. These taxa were correlated with 376 metabolites ($p<0.05$) with enrichment in fatty acid biosynthesis, linoleic/arachidonic acid metabolism, and propanoate metabolism pathways. They were also associated with 146 proteins ($p<0.001$) with enrichment in PI3K-Akt signalling, ECM-receptor interaction, and lipid/atherosclerosis pathways.*

### Conclusion

*$OB^+OA^+$ patients exhibited significant gut microbial dysbiosis associated with systemic metabolic and proteomic alterations relevant to OA pathophysiology. The microbiome-metabolome-proteome axis may provide mechanistic insights into worsened OA outcomes in OB individuals and could inform microbiome-targeted interventions.*

**Key words**

knee osteoarthritis, obesity, gut microbiomics, metabolomics, proteomics, ontegrative analysis

*Jingyi Huang, BSc*
*Ming Liu, MSc*
*Hongwei Zhang, MSc*
*Guang Sun, PhD*
*Andrew Furey, MD*
*Proton Rahman, MD*
*Guangju Zhai, PhD*

*Please address correspondence to:*
*Guangju Zhai*
*Human Genetics & Genomics,*
*Division of BioMedical Sciences,*
*Faculty of Medicine,*
*Memorial University of Newfoundland,*
*St. John's,*
*Newfoundland and Labrador,*
*A1B 3V6 Canada.*
*E-mail: gzhai@mun.ca*

*Received on October 24, 2025; accepted in revised form on December 19, 2025.*



*ORCID iD*
*J. Huang: 0009-0004-4466-4156*
*M. Liu: 0000-0001-7745-448X*
*H. Zhang: 0009-0005-8263-3147)*
*G. Sun: 0000-0003-4300-0134*
*A. Furey: 0000-0001-7748-8751*
*P. Rahman: 0000-0002-4521-2029*
*G. Zhai: 0009-0005-0088-6838*

*Funding: the NFOAS was funded by the Canadian Institutes of Health Research (FRN no. 175015; 153298; 143058; 132178; 191966), Arthritis Society Canada (ID no. 22-121), the Research and Development Corporation of Newfoundland and Labrador (5404.1423.102), and Memorial University of Newfoundland Medical Research Fund. The CODING study was funded by the Canadian Institutes of Health Research (MOP192552).*

*Competing interests: none declared.*

## Introduction

Osteoarthritis (OA) is the most common form of arthritis in adults, with a global prevalence of approximately 7.6% reported in 2020 (1). Multiple factors including age, sex, obesity (OB), genetic predisposition, and joint injury contribute to the development of OA (2). Among these, excess body weight is a major modifiable risk factor, particularly for knee OA (3). Individuals with OB are more than twice as likely to develop knee OA compared to those with a normal weight (4). Furthermore, Mendelian randomisation (MR) studies have provided strong evidence supporting a causal relationship between OB and knee/hip OA (5).

OB-related OA represents a substantial proportion of the clinical OA population, yet studies specifically addressing this phenotype remain limited. Increased expression of cytokines, metalloproteinases, and inflammation-related genes have been observed in OB-induced OA mouse (6). However, corresponding studies in human subjects are scarce. Elevated fatty acid-binding protein 4 (FABP4) levels have been reported in obese female OA patients (7), while higher baseline fibulin-3 levels were associated with the incidence of knee OA in middle-aged overweight and obese women (8). Despite the evidence that obese individuals exhibit severely disturbed plasma metabolome and proteome (9), most previous studies on OB-related OA only focused on a small number of biomarkers. To address this gap, our lab recently conducted a metabolome-wide analysis specifically targeting OB-related knee OA. This study identified lower levels of acyl-alkyl-phosphatidylcholine C40:6 (PC ae C40:6) as being associated with increased risk of OB-related knee OA, higher body mass index (BMI) at 10-year follow-up, as well as the incidence of radiographic and symptomatic knee OA at 5-year follow-up (10).

Given that host metabolomic and proteomic alterations are often shaped by the gut microbiota (11), these findings prompted us to explore the gut microbiome as a potential upstream driver of OB-related knee OA. A number of studies have highlighted the roles of gut microbiota in the development of both OA and OB. Several microbial taxa, including *Streptococcus* and *Bacteroides*, were found to be positively or negatively associated with OA (12). It has also been reported that bacterial products such as short-chain fatty acids (SCFAs) could protect joint and slow the progression of OA by enhancing intestinal barrier integrity, suppressing systemic inflammation, and maintaining joint homeostasis (13). In addition, gut microbiota has been shown to increase caloric harvest, modulate appetite, and regulate fat storage and insulin sensitivity in the host (14), contributing to weight gain. Therefore, we hypothesised that gut microbiota-induced alterations on metabolomic and proteomic levels may also contribute to the development of OB-related knee OA. The aim of the current study was to investigate gut microbial alteration and its functional consequences in OB-related knee OA, with the ultimate goal being informing more precise and personalised intervention strategies, such as dietary modification and probiotic supplementation.

## Methods

*Study participants*

The current study was conducted as part of the ongoing Newfoundland Osteoarthritis Study (NFOAS), which recruited OA patients between November 2011 and September 2017 at St Clare's Mercy Hospital and Health Sciences Centre General Hospital in St John's, Newfoundland & Labrador (NL), Canada (16). OA diagnosis was based on the American College of Rheumatology OA clinical diagnostic criteria (17) and was confirmed by the attending orthopaedic surgeon, as well as the pathology reports on the replaced joints. OA-free controls derived from a previous study, the Complex Diseases in the Newfoundland population: Environment and Genetics (CODING) study (18), which recruited participants from the same source population in NL. Individuals with no clinically diagnosed or self-reported OA in any joint were defined as controls. OB was defined as BMI≥30 kg/m$^2$.

Ethics approval for this study was obtained from the Health Research Eth-

ics Authority of Newfoundland and Labrador (HREB no. 2011.311 and no. 2017.121). All study participants provided written informed consent prior to enrolment.

*Data and sample collection*

For fecal sample and dietary intake data collection, an OMNIgene•GUT collection kit (DNA Genotek, Ottawa, Canada) and two questionnaires were mailed to each participant. Each kit contained detailed user instructions, a spatula, a collection tubes pre-filled with DNA preservation solution, a bio-specimen bag, and toilet accessories. The DNA preservation solution was able to maintain DNA integrity at room temperature for up to 60 days or at -80 °C for up to one year. The questionnaires collected information on dietary intake pattern within the 12 months and antibiotic use within the three months prior to fecal sample collection, respectively (Full questionnaires are provided in the online Supplementary file). Participants were instructed to complete the questionnaires, collect their fecal sample according to the manufacturer's instructions to minimise contamination, record the collection date and time, and then return the sample tube and questionnaires to the laboratory.

Upon receipt, 1 ml of each fecal sample was immediately aliquoted into a sterile screw-cap vial and stored at -80 °C until analysis. The average time from sample collection to freezing was 9±8.3 days. Metagenomic DNA was extracted using the QIAGEN PowerSoil DNA Kit (QIAGEN, Hilden, Germany) following the manufacturer's instructions. DNA quality was assessed using a Qubit fluorometer and DNA samples were stored at -20°C until microbiome analysis.

Sequencing libraries were prepared with the Illumina DNA Prep kit (Illumina, San Diego, USA). Starting with 1 ng of DNA per sample, the process included enzymatic shearing and adaptor tagging, PCR amplification with barcode integration, purification by beads, and normalisation using Illumina beads approach. The V4-V5 variable region of the 16S rRNA gene was amplified with Phusion High-Fidelity DNA polymerase (Thermo Fisher Scientific, Waltham, USA) using primers 515FB (GTGYCAGCMGCCGCGGTAA) and 926R (CCGYCAATTYMTTTRAGTTT), each containing sample-specific barcodes. PCR products were then verified on Coastal Genomics Analytical Gels (Coastal Genomics, Burnaby, Canada). Amplicons were cleaned and normalised with the Charm Biotech Just-a-Plate 96-well Normalization Kit (Charm Biotech, Cape Girardeau, USA). Finally, sequencing of the 16s rRNA gene V4-V5 region was performed on the Illumina MiSeq i100 platform using 300+300 bp paired-end reads with XLEAP chemistry at the Integrated Microbiome Resource (Dalhousie University, Halifax, Canada).

Fasting plasma samples were used for both metabolomic and proteomic profiling. Metabolomic profiling was performed using the Biocrates MxP Quant 500 Kit (BIOCRATES Life Sciences AG, Innsbruck, Austria), which quantifies up to 630 different endogenous metabolites. A full list of the measured metabolites is provided in Supplementary Table S1. The profiling was performed on an API5500 Qtrap® tandem mass spectrometry instrument (Applied Biosystems/MDS Analytical Technologies, Foster City, USA) coupled with a liquid chromatography at The Metabolomic Innovation Centre (TIMC; https://metabolomicscentre.ca). The Biocrates MetIQ software was used to manage the entire assay workflow from sample registration and automated calculation of metabolite concentrations to the data export for downstream analysis. Metabolite concentrations were reported as μMol/L.

Proteomic profiling was performed using the Olink® Explore HT platform (Olink®, Uppsala, Sweden), which quantifies more than 5,400 proteins with >99% specificity. A complete list of the measured proteins is provided in Supplementary Table S2. Proteomic profiling was conducted at the McGill Genome Centre (https://www.mcgill-genomecentre.ca) following the manufacturer's standard protocol. Each sample included three internal controls (extension, incubation, and amplification). The extension control was used for normalisation and calculation of normalised protein eXpression (NPX) values, while the incubation and amplification controls monitored assay performance and technical integrity. Each assay plate also included three external controls: a plate control (pooled human plasma) for data normalisation and quality control (QC) of each run, a sample control to assess potential variation between runs, and a negative control (buffer) to detect any unexpected signals. Data QC and analysis were performed using Olink® NPX Manager software, and protein levels were reported as NPX values.

*Statistical analyses*

Gut microbial sequencing data were processed using the Microbiome Helper pipeline based on QIIME2 (https://github.com/LangilleLab/microbiome_helper). Amplicon Sequence Variants (ASVs) were generated using Deblur(19). Within-sample α-diversity was estimated using Shannon, Simpson, Chao1, and Abundance-based coverage estimators (ACE) indices, while between-sample β-diversity was assessed using Bray-Curtis dissimilarity and visualised by principal coordinate analysis (PCoA). Statistical significance of α-diversity measures was assessed using analysis of covariance (ANCOVA) with age, sex, and antibiotic use as covariates. Group differences in β-diversity were evaluated using permutational multivariate analysis of variance (PERMANOVA), also adjusting for age, sex, and antibiotic use. To identify taxonomic differences across the four defined subgroups ($OB^+OA^+$, $OB^-OA^+$, $OB^+OA^-$, and $OB^-OA^-$), we applied Microbiome Multivariable Association with Linear Models 2 (MaAsLin2) with zero-inflated negative binomial (ZINB) model, adjusting for age and sex. Statistical significance level was set at $\alpha=7.65\times10^{-5}$ to control for multiple testing for 654 ASVs with Bonferroni correction method. Antibiotic use and dietary intake were then incorporated into the models stepwise to examine their effects on OB/OA outcomes. Functional metagenomic predictions were performed with Phylogenetic Investigation of Communities by Reconstruction of Unobserved States

**Table I.** Characteristics of the study participants.

| | $OB^+OA^+$ n=66 | $OB^-OA^+$ n=25 | $OB^+OA^-$ n=5 | $OB^-OA^-$ n=7 | P[1] | P[2] | P[3] |
|---|---|---|---|---|---|---|---|
| Age (years) | 61.6 ± 4.9 | 65.2 ± 6.1 | 52.2 ± 8.0 | 54.1 ± 4.6 | 0.01 | $4.82\times10^{-3}$ | $5.35\times10^{-4}$ |
| BMI ($kg/m^2$) | 36.5 ± 5.2 | 27.2 ± 1.9 | 33.3 ± 3.0 | 27.6 ± 1.8 | $<2\times10^{-16}$ | 0.15 | $1.23\times10^{-9}$ |
| Sex: female (n) | 46 | 12 | 4 | 6 | 0.09 | 0.51 | 0.67 |
| Antibiotics use (n) | 14 | 0 | 2 | 1 | 0.02 | 0.60 | 1™ |

Values are either mean ± standard deviation or counts. *p*-values were obtained using Student's t-test or Wilcoxon rank-sum test for continuous variables (age and BMI) and Chi-squared test or Fisher's exact test for categorical variables (sex and antibiotic use), as appropriate. For antibiotic data, 57/66 $OB^+OA^+$ patients, 21/25 $OB^-OA^+$ patients, and all non-OA patient completed the questionnaire. P1: $OB^+OA^+$ *vs*. $OB^-OA^+$; P2: $OB^+OA^+$ *vs*. $OB^+OA^-$; P3: $OB^+OA^+$ *vs*. $OB^-OA^-$

(PICRUSt2)(20), which infers the functional potential of microbial communities by placing sequences and relative abundances into a reference phylogenetic tree and leveraging an expanded genomic database with improved gene and pathway prediction algorithms.

For metabolomics, metabolites with values below the limit of detection (LOD) in more than 25% of the samples were excluded. For the remaining metabolites, values <LOD were imputed using a linear regression model in which concentration of a given metabolite was regressed on age, sex, and BMI. Principal component analysis (PCA) revealed no batch effect. A total of 622 metabolites passed QC and were included in subsequent analysis. For proteomics, data points were excluded if they showed insufficient total read counts, abnormal or unbalanced internal control signals, unexpected signals in negative controls, or deviations from the expected signal pattern of external controls. A total of 5,416 proteins were assessed, all of which passed QC and were included in the analysis. Associations between metabolite, protein, and the identified microbes were evaluated using Spearman correlation. Metabolite pathway enrichment was performed in MetaboAnalyst 6.0 (https://www.metaboanalyst.ca). Protein functional enrichment was assessed using Kyoto Encyclopedia of Genes and Genomes (KEGG) (21) and Gene Ontology (GO) (22) databases.

Dietary patterns were categorised into the following 11 main food categories: white meat, red meat, processed meat, plant-based protein, dairy products, fruits, vegetables, refined carbohydrates and sweets, grains and cereals, beverages, and nuts and seeds (Details of the components included in each category are provided in Suppl. Table S3). The frequency of consumption for each food category was ranked into quartiles, and participants were assigned accordingly. To examine whether the dietary intake influenced the significant microbial taxa, food intake frequency was incorporated into the model with adjustment for age, sex, and antibiotic use. Dietary intake frequencies were categorised into quartiles with quartile 1 was set as reference, and associations were considered indicative of dietary influence only when quartiles 2 to 4 all showed statistically significant associations in the same direction.

Statistical significance was evaluated using Student's *t*-test or Wilcoxon rank-sum test for continuous variables and Chi-squared test or Fisher's exact test for categorical variables, as appropriate. All statistical analyses and visualisation were performed in R v. 4.3.2 with vegan (23), picante (24), ggplot2 (25), Maaslin2 (26), phyloseq (27), ggpicrust2 (28) packages.

## Results

*Participants' characteristics*

A total of 91 patients with knee OA and 12 OA-free controls were included in this exploratory study and classified into four subgroups based on OA and OB status: $OB^+OA^+$ (n=66), $OB^-OA^+$ (n=25), $OB^+OA^-$ (n=5), and $OB^-OA^-$ (n=7). The $OB^+OA^+$ group was younger than $OB^-OA^+$ but older than both non-OA subgroups. In addition, the $OB^+OA^+$ group had a significantly higher proportion of female participants and a greater number of individuals with a history of antibiotic use within the three months prior to fecal sample collection compared with the $OB^-OA^+$ group (all $p<0.05$; details in Table I and Suppl. Table S4).

*Diversity of the gut microbiome*

Sequencing of the16S rRNA V4-V5 region yielded a total of 6,119,490 paired-end reads, with an average of 59,413 reads per sample. ASVs present in less than 10% of samples were excluded, resulting in 654 ASVs for downstream analyses, encompassing 8 phyla, 14 classes, 30 orders, 52 families, and 153 genera.

α-diversity was assessed using diversity indices (Shannon and Simpson) and richness estimators (Chao1 and ACE) with adjustment for age, sex, and antibiotic use. Patients in the $OB^+OA^+$ group exhibited lower α-diversity compared with $OB^-OA^+$ (all $p<0.05$) except for Simpson index ($p=0.27$). No significant differences were observed among the other three subgroups. In addition, $OB^+OA^+$ patients showed borderline lower Chao1 and ACE in α-diversity compared with $OB^+OA^-$ and $OB^-OA^-$ ($p=0.052$-$0.07$) (Fig. 1A). Both indices are primarily sensitive to species richness, suggesting a trend toward reduced microbial richness in the $OB^+OA^+$ subgroup. β-diversity, evaluated using Bray-Curtis dissimilarity, showed that the first two principal coordinates explained 15.17% of the variation in microbial composition. Pairwise PERMANOVA with adjustment for age, sex, and antibiotic use indicated that the microbial communities in the $OB^+OA^+$ group were significantly different from those in $OB^-OA^+$ and $OB^-OA^-$ groups, whereas no significant differences were observed among the other subgroup comparisons (Fig. 1B). Although the $OB^+OA^+$ group had a higher proportion of individuals with a recent history of

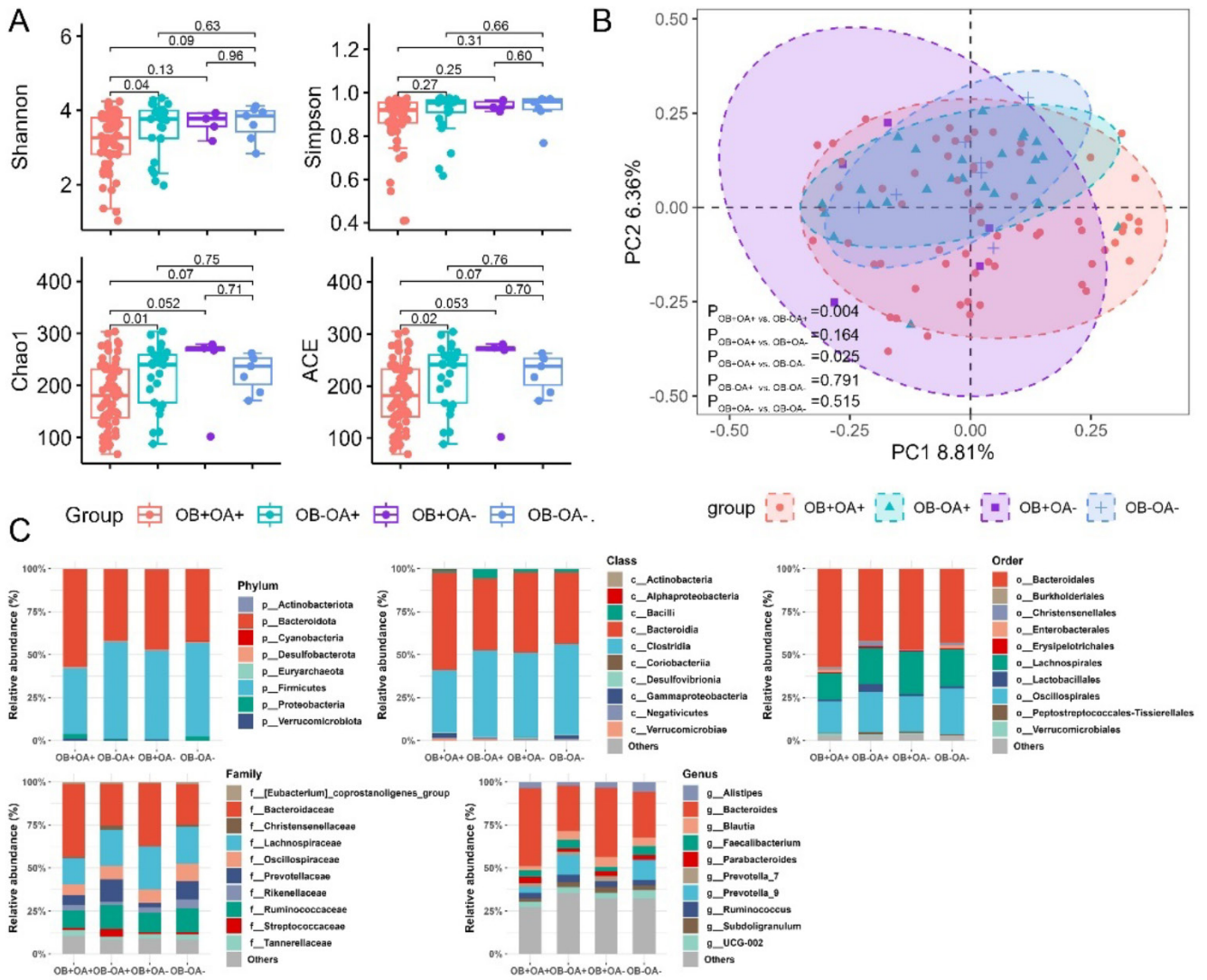


**Fig. 1. A**: Differences in α-diversity between four OA/OB subgroups assessed by Shannon, Simpson, Chao1, and ACE indices. Significance was evaluated using analysis of covariance (ANCOVA) with adjustment for age, sex, and antibiotic use history.
**B**: β-diversity differences between the four OA/OB subgroups were estimated by Principal coordinates analysis (PCoA) based on Bray-Curtis distance. Significance was evaluated using Permutational Multivariate Analysis of Variance (PERMANOVA) with adjustment for age, sex, and antibiotic use history.
**C**: The proportions of bacteria at different taxonomic levels in each subgroup. At the order, family, and genus levels, the subfigures only displayed the top 10 most abundant bacteria.

antibiotic use compared with the $OB^-OA^+$ group, adjusting for antibiotic exposure did not eliminate the observed differences in diversity.

*Differences in microbial abundances*

Relative abundance stack plots demonstrated that *Bacteroidota* and *Firmicutes* were the predominant phyla across all groups. At the class level, *Bacteroidia*, *Clostridia*, and *Bacilli* were the most abundant taxa, while at the order level, communities were primarily composed of *Bacteroidales*, *Oscillospirales*, *Lachnospirales*, and *Lactobacillales*. Wilcoxon rank-sum testing revealed that the $OB^+OA^+$ group had a lower abundance of *Peptostreptococcales-Tissierellaless* compared with $OB^-OA^+$ ($p$=1.27×10$^{-3}$). At the family level, *Barnesiellaceae*, *Lachnospiraceae*, *Ruminococcaceae,* *Prevotellaceae*, and *Oscillospiraceae* were dominant, and $OB^+OA^+$ had a lower abundance of *Peptostreptococcaceae* compared with $OB^-OA^+$ ($p$=1.62×10$^{-4}$). Detailed taxonomic profiles at each level are presented in Figure 1C.

Taxa ratios were compared between subgroups. Relative abundances of taxa with the same name at the same taxonomic level were summed, and ratios were calculated between these values. At the phylum level, $OB^+OA^+$ displayed higher *Proteobacteria*/*Euryarchaeota*, *Proteobacteria*/*Firmicutes*, and *Proteobacteria*/*Actinobacteriota* ratios than $OB^-OA^+$ (all $p$<8.93×10$^{-4}$). At the class level, $OB^+OA^+$ exhibited a higher *Gammaproteobacteria*/*Methanobacteria* ratio compared with $OB^-OA^+$ ($p$=1.92×10$^{-4}$).

MaAsLin2 with ZINB model, adjusted for age and sex, identified four taxa with significant differences between $OB^-OA^+$ and $OB^+OA^+$, seven between $OB^+OA^-$ and $OB^+OA^+$, and six between $OB^-OA^-$ and $OB^+OA^+$ (all $p$<7.65×10$^{-5}$ after correction for 654 ASVs). The taxon most positively associated with $OB^+OA^+$ was *Muribaculaceae* ($p$=4.51×10$^{-7}$; β=8.8

**Table II.** Results from the microbiome multivariable association with linear models (MaAsLin2) analyses.

| | Taxonomy | Model 1 | | Model 2 | |
|---|---|---|---|---|---|
| | | β±SD | *p*-value | β±SD | *p*-value |
| $OB^-OA^+$ *vs.* $OB^+OA^+$ | d_Bacteria; p_Bacteroidota; c_Bacteroidia; o_Bacteroidales; f_Rikenellaceae; g_Alistipes_1; | 2.14 ± 0.33 | $1.29\times10^{-10}$ | 2.30 ± 0.38 | $1.54\times10^{-9}$ |
| | d_Bacteria; p_Firmicutes; c_Clostridia; o_Oscillospirales; f_Ruminococcaceae; g_Angelakisella; | 5.29 ± 1.08 | $1.01\times10^{-6}$ | 5.34 ± 1.11 | $1.45\times10^{-6}$ |
| | d_Bacteria; p_Proteobacteria; c_Gammaproteobacteria; o_Enterobacterales; f_Pasteurellaceae; g_Haemophilus; | 3.02 ± 0.65 | $3.68\times10^{-6}$ | 2.55 ± 0.83 | $2.13\times10^{-3}$ |
| | d_Bacteria; p_Firmicutes; c_Clostridia; o_Lachnospirales; f_Lachnospiraceae_1; | 6.46 ± 1.46 | $1.01\times10^{-5}$ | *6.45 ± 1.57 | $*4.09\times10^{-5}$ |
| $OB^+OA^-$ *vs.* $OB^+OA^+$ | d_Bacteria; p_Firmicutes; c_Clostridia; o_Christensenellales; f_Christensenellaceae; g_Christensenellaceae_R-7_group; | -1.44 ± 0.28 | $2.38\times10^{-7}$ | -1.50 ± 0.25 | $2.31\times10^{-9}$ |
| | d_Bacteria; p_Firmicutes; c_Clostridia; o_Oscillospirales; f_Ruminococcaceae_1; | 3.40 ± 0.71 | $1.45\times10^{-6}$ | 3.91 ± 0.56 | $3.52\times10^{-12}$ |
| | d_Bacteria; p_Firmicutes; c_Clostridia; o_Lachnospirales; f_Lachnospiraceae_2; | -5.13 ± 1.12 | $4.78\times10^{-6}$ | -2.29 ± 1.25 | 0.06 |
| | d_Bacteria; p_Firmicutes; c_Clostridia; o_Oscillospirales; f_Ruminococcaceae_2; | 3.52 ± 0.78 | $6.23\times10^{-6}$ | 4.27 ± 0.93 | $4.63\times10^{-6}$ |
| | d_Bacteria; p_Firmicutes; c_Clostridia; o_Oscillospirales; f_Ruminococcaceae; g_Faecalibacterium; | 6.97 ± 1.60 | $1.24\times10^{-5}$ | 6.53 ± 1.88 | $5.17\times10^{-4}$ |
| | d_Bacteria; p_Firmicutes; c_Clostridia; o_Oscillospirales; f_Butyricicoccaceae; g_Butyricicoccus; | 2.61 ± 0.62 | $2.92\times10^{-5}$ | *2.85 ± 0.60 | $*2.20\times10^{-6}$ |
| | d_Bacteria; p_Firmicutes; c_Clostridia; o_Oscillospirales; f_Ruminococcaceae; g_Ruminococcus; | -11.35 ± 2.75 | $3.58\times10^{-5}$ | -11.33 ± 3.00 | $1.62\times10^{-4}$ |
| $OB^-OA^-$ *vs.* $OB^+OA^+$ | d_Bacteria; p_Bacteroidota; c_Bacteroidia; o_Bacteroidales; f_Rikenellaceae; g_Alistipes_2; | 6.89 ± 1.06 | $8.66\times10^{-11}$ | *3.24 ± 1.53 | *0.03 |
| | d_Bacteria; p_Bacteroidota; c_Bacteroidia; o_Bacteroidales; f_Muribaculaceae; g_Muribaculaceae; | 8.85 ± 1.75 | $4.51\times10^{-7}$ | *7.33 ± 1.04 | $*2.26\times10^{-12}$ |
| | d_Bacteria; p_Bacteroidota; c_Bacteroidia; o_Bacteroidales; f_Bacteroidaceae; g_Bacteroides; | 5.65 ± 1.23 | $3.97\times10^{-6}$ | 7.02 ± 1.09 | $1.17\times10^{-10}$ |
| | d_Bacteria; p_Firmicutes; c_Clostridia; o_Lachnospirales; f_Lachnospiraceae; g_Anaerostipes; | 4.05 ± 0.94 | $1.59\times10^{-5}$ | *5.19 ± 0.67 | $*1.15\times10^{-14}$ |
| | d_Bacteria; p_Firmicutes; c_Bacilli; o_Erysipelotrichales; f_Erysipelatoclostridiaceae; g_Erysipelatoclostridium; | 3.99 ± 0.97 | $3.74\times10^{-5}$ | *2.73 ± 1.16 | *0.02 |
| | d_Bacteria; p_Bacteroidota; c_Bacteroidia; o_Bacteroidales; f_Prevotellaceae; g_Prevotella_7; | 7.12 ± 1.80 | $7.31\times10^{-5}$ | 6.73 ± 3.26 | $3.90\times10^{-2}$ |

In Model 1, *p*-values were obtained using MaAsLin2 with a zero-inflated negative binomial (ZINB) model, adjusted for age and sex.
In Model 2, *p*-values were obtained with additional adjustment for antibiotic use. Furthermore, for results marked with an asterisk (*), we further adjusted for the dietary factors significantly associated with those taxa. The β±SD values represent the coefficients and standard deviation for the $OB^+OA^+$ group.

in $OB^-OA^-$ *vs.* $OB^+OA^+$ comparison), while the strongest negative association was observed for *Ruminococcus* ($p=3.56\times10^{-5}$; β=-11.3 in $OB^+OA^-$ *vs.* $OB^+OA^+$ comparison). Details of all comparisons are provided in Table II.

Analysis of dietary influence revealed that that processed meat consumption was negatively associated with *Lachnospiraceae* abundance, vegetable consumption was negatively associated with *Muribaculaceae*, fruit consumption was positively associated with *Anaerostipes*, and beverage consumption was positively associated with *Alistipes*. In addition, red meat intake was positively associated with *Erysipelatoclostridium* abundance, while *Butyricicoccus* showed a negative association with the consumption of refined carbohydrates and sweets (all $p<0.05$).

After incorporating dietary intake into the models, along with age, sex, and antibiotic use, 16 out of 17 bacterial taxa remained significant (all $p<0.05$). However, *Lachnospiraceae_2* was no longer significant between $OB^+OA^-$ and $OB^+OA^+$ ($p=0.067$).

In addition, PICRUSt2 functional predictions were performed on both the 16 identified taxa and whole metagenome. Analysis of the 16 identified taxa predicted an upregulation of primary and secondary bile acid biosynthesis in the $OB^+OA^+$ group (Fig. 2A). Predictions on the whole metagenome revealed an upregulation of glycosphingolipid biosynthesis, glycosaminoglycan degradation, and lipopolysaccharide (LPS) biosynthesis pathways in $OB^+OA^+$ (Fig. 2B).

### *Association between the identified microbial taxa and plasma metabolites and proteins*

Spearman correlation analysis identified 376 metabolites to be correlated with the 16 taxa that remained significant after adjustment for dietary factors, age, sex, and antibiotic use ($p<0.05$) (Suppl. Table S5).

Metabolite enrichment analysis was performed in MetaboAnalyst 6.0 for each set of microbe-associated metabolites. *Ruminococcaceae*-associated metabolites were enriched in pathways related to unsaturated fatty acids biosynthesis, as well as linoleic acid and arachidonic acid metabolism. *Muribaculaceae*-associated metabolites were enriched in the propanoate metabolism and alanine, aspartate and glutamate metabolism pathways. *Alistipes*-associated metabolites were enriched in sphingolipid metabolism and linoleic acid metabolism (Fig. 3A, details in Suppl. Table S6).

Proteomic data were available for 13 $OB^+OA^+$ and 22 $OB^-OA^+$ patients. Spearman correlation analysis revealed that 146 proteins were associated with

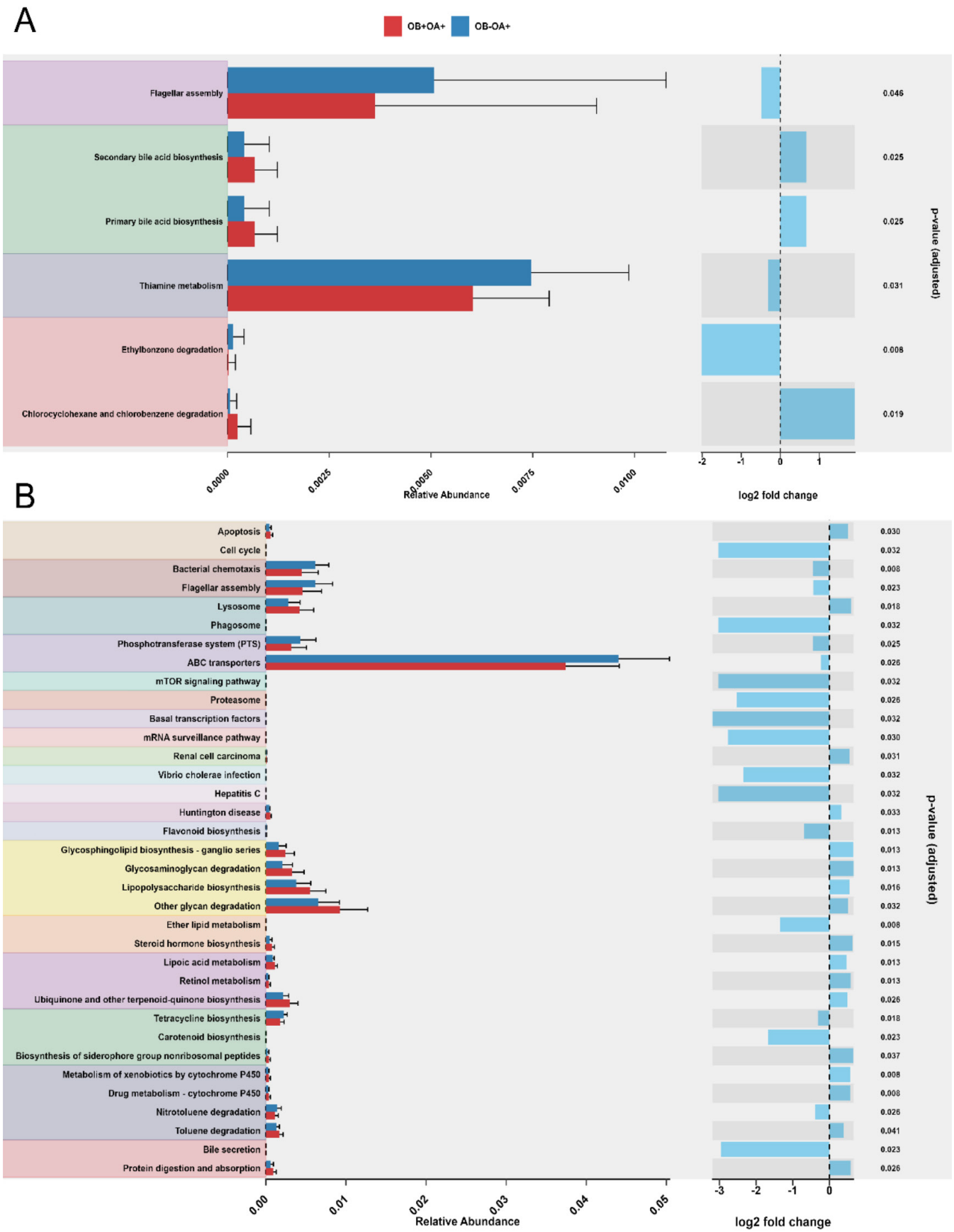


**Fig. 2.** PICRUSt2 identified potential functional pathways that differed between the $OB^{+}OA^{+}$ and $OB^{-}OA^{+}$ based on sequencing and abundance. **A**: PICRUSt2 functional prediction based on the 16 identified taxa. **B**: PICRUSt2 functional prediction based on whole metagenome.

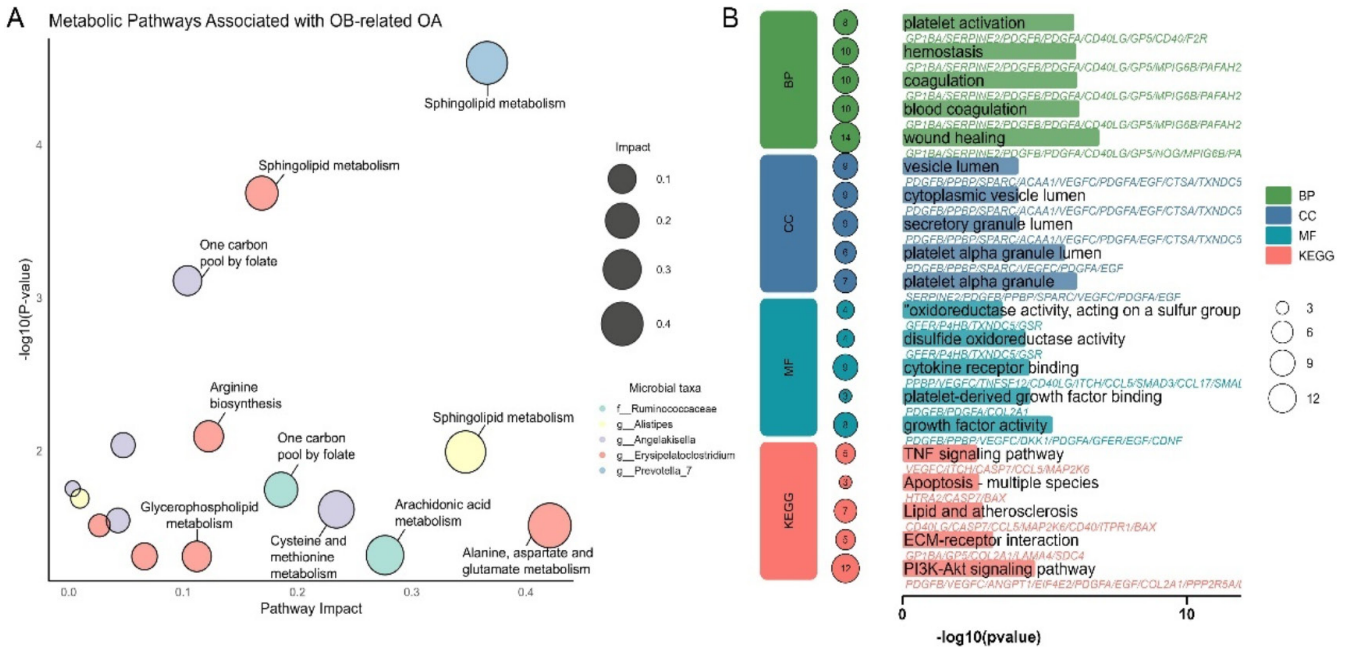


**Fig. 3.** Metabolic pathway, Kyoto Encyclopedia of Genes and Genomes (KEGG) and Gene Ontology (GO) enrichment analyses result.
**A**: Metabolic pathway results of metabolites associated with OB-related OA-associated microbial taxa.
**B**: GO and KEGG enrichment result of *Erysipelatoclostridium*-associated proteins.

the 16 taxa ($p$<0.001), of which 110 were linked to *Erysipelatoclostridium* (all correlations with $p$<0.05 are provided in Suppl. Table S7). KEGG and GO enrichment analyses of these 110 proteins indicated significant involvement of the PI3K-Akt signalling pathway, ECM-receptor interaction, and TNF signalling pathway (Fig. 3B).

## Discussion

This exploratory study provided integrative evidence linking gut microbial signatures with metabolomic and proteomic alterations and dietary factors in OB-related knee OA. We observed that patients with both OB and OA exhibited reduced microbial α- and β-diversity compared with non-obese OA patients, together with specific taxonomic shifts, including the most enrichment of *Muribaculaceae* and depletion of *Ruminococcus*. These microbial signatures correlated with distinct plasma metabolites and proteins involved in lipid metabolism, inflammation, and extracellular matrix (ECM) regulation. Taken together, these findings highlighted a potential mechanistic axis between gut microbiome, systemic metabolic pathways, and OA pathophysiology, particularly in the setting of OB.

Reduced microbial α-diversity has been widely reported in OB and is often considered as a hallmark of gut dysbiosis (29). In the current study, $OB^+OA^+$ patients had significantly lower α-diversity compared with $OB^-OA^+$. Although not statistically significant, $OB^+OA^+$ patients also demonstrated a trend towards lower α-diversity in richness compared with non-OA groups, raising the possibility that OA itself may also contribute to gut microbial dysbiosis. This interpretation is consistent with previous studies reporting gut dysbiosis in OA patients (30), although evidence remained inconclusive (31).

*Muribaculaceae* was the taxon most strongly and positively associated with $OB^+OA^+$ patients. This finding appeared to contrast with those in mouse studies, where increased *Muribaculaceae* abundance has been associated with the alleviation of OB (32), and its reduction was observed in the destabilisation of the medial meniscus (DMM) mouse model of OA (33). However, as existing evidence primarily comes from animal models, further research is needed to clarify the role of *Muribaculaceae* in human patients.

The potential role of *Muribaculaceae* may be explained by its metabolic functions. This bacterial family degrades complex plant polysaccharides to produce SCFAs such as butyrate and propionate (32). Butyrate has been shown to protect against OA by regulating autophagy and inflammatory cell death of chondrocytes (34). Similarly, indole-3-propionic acid (IPA) (microbial metabolite produced from propanoate metabolism) has been shown to alleviate chondrocyte inflammation and extracellular matrix degradation by inhibiting the NF-κB signalling pathway(35). Consistent with this, we observed enrichment of *Muribaculaceae*-associated metabolites within the propanoate metabolism pathway (Suppl. Table S6), suggesting that the increased abundance of *Muribaculaceae* in $OB^+OA^+$ patients may represent a compensatory response to gut dysbiosis. Thus, elevated *Muribaculaceae* abundance could reflect an adaptive microbial attempt to restore metabolic homeostasis through enhanced SCFA production.

In contrast, *Ruminococcus* displayed the strongest negative association with $OB^+OA^+$. This negative association was significant when compared with the $OB^+OA^-$ group, and was also observed, though not significant after multiple testing correction, when compared with the $OB^-OA^+$ group. Notably, decreased abundance of *Ruminococcus* has been consistently reported in human studies

of OA patients compared with controls (30). This raised the possibility that *Ruminococcus* depletion may contribute to OA pathogenesis in the presence of OB, potentially by diminishing the capacity for fiber fermentation and SCFA production (36).

*Alistipes* abundance demonstrated a gradient enrichment, being significantly higher in $OB^+OA^+$ compared with $OB^-OA^-$ ($\beta$=6.6, $p$=8.66×$10^{-11}$), $OB^+OA^-$ ($\beta$=4.1, $p$=0.002), and $OB^-OA^+$($\beta$=2.1, $p$=1.29×$10^{-10}$) groups. This pattern suggested that *Alistipes* may respond to the cumulative burden of metabolic and joint disease. Furthermore, we observed a positive association between beverage consumption (including coffee and alcohol) and *Alistipes* abundance. Both caffeine and alcohol intake have previously been reported to increase *Alistipes* levels (37, 38). Importantly, these exposures may contribute to joint pathology: caffeine can inhibit the expression of cartilage matrix genes such as collagen type II alpha 1 chain (*COL2A1*) and aggrecan (*ACAN*), thereby promoting chondrocyte degeneration (39); excessive alcohol consumption has been linked to the loss of cartilage proteoglycans and increased risk of knee OA (40). Furthermore, *Alistipes* has been associated with pro-inflammatory activity through toll like receptor-4 (TLR4) activation and tumour necrosis factor (TNF) production (41). Together, these findings suggested that elevated *Alistipes*, in conjunction with higher caffeine and alcohol intake in $OB^+OA^+$ patients, may contribute to the disease development via pro-inflammatory pathways and impaired cartilage homeostasis.

However, the association between *Alistipes* and OA appears to vary across populations. A study in British participants reported increased *Alistipes* abundance in OA (42), whereas research in a Chinese cohort found decreased levels in overweight OA patients (43). The NL population examined in the current study is primarily descended from Irish and English settlers, and the discrepancies across studies may reflect population-specific host-microbiome interactions. These observations highlighted the importance of ancestral, dietary, and environmental factors when evaluating microbiome-based biomarkers and potential therapeutic targets.

In addition to *Alistipes*, *Erysipelatoclostridium* emerged as another notable taxon positively associated with the $OB^+OA^+$ group. In proteomic correlation analyses, this genus accounted for the majority of the significant correlations, suggesting its central role in shaping host molecular responses. Previous mouse studies have shown that *Erysipelatoclostridium* can promote high-fat diet-induced OB by enhancing the transcription of glucose transporter 2 (Glut2) and fatty acid translocase (CD36) mRNA (44). However, its role in OA pathogenesis has remained poorly understood. Our findings revealed that *Erysipelatoclostridium*-associated proteins were significantly enriched in the PI3K-Akt signalling pathway (Fig. 3B). This pathway is well established in OA pathogenesis, where it drives cartilage matrix degradation, synovial inflammation, and subchondral bone dysfunction (45). In addition, TNF signalling pathway and apoptosis pathway were also associated *Erysipelatoclostridium*. TNF-$\alpha$ inhibition has been shown to alleviate inflammation by downregulating the PI3K-Akt signalling pathway in mouse model (46). The PI3K-Akt signalling pathway also participates in the regulation of chondrocyte apoptosis (45). Thus, *Erysipelatoclostridium* or its metabolic products may influence joint pathology through the modulation of PI3K-Akt signalling, but the causality needs further experimental validation, particularly to determine whether microbial metabolites directly activate this pathway in joint tissues and systemic inflammation.

Dietary analysis provided additional context: red meat consumption was positively correlated with *Erysipelatoclostridium* abundance. Red meat intake is known to increase bile acid production, particularly deoxycholic acid (DCA), and long-term exposure to DCA has been shown to activate the PI3K-Akt signalling pathway in colonic cells (47). In addition, *Erysipelotrichaceae* has been reported to participate in bile acid metabolism through the production of bile salt hydrolase (48), and bile acids could activate TNF-$\alpha$ and IL-1$\beta$ signalling pathways to exert pro-inflammatory effects (49). PICRUSt2 also suggested that the primary and secondary bile acid biosynthesis pathways were upregulated in $OB^+OA^+$ group. This observation suggested a potential diet-microbe-host signalling axis, whereby red meat-driven expansion of *Erysipelatoclostridium* could amplify OA-related molecular pathways via bile acid metabolism and PI3K-Akt activation.

Furthermore, in the PICRUSt2 predictions based on the whole metagenome, we observed that glycosaminoglycan degradation and LPS biosynthesis pathways were upregulated in the $OB^+OA^+$ group. The degradation of glycosaminoglycans in the extracellular matrix of cartilage is considered an early landmark of the OA pathogenesis, contributing to diminished cartilage resilience and progressive joint deterioration (50). This microbial functional signature therefore mirrors one of the central pathogenic processes in OA. In parallel, enhanced microbial capacity for LPS biosynthesis provided a potential mechanistic link between OB-associated dysbiosis and OA progression. Circulating LPS levels are elevated in OB individuals through multiple mechanisms, including increased intestinal permeability and shifts in gut microbial composition (51). Elevated systemic LPS can activate TLR4-mediated inflammatory pathways, thereby promoting low-grade systemic inflammation and accelerating OA-related joint damage (51). Together, these findings suggested that the gut microbiome in $OB^+OA^+$ patients may contribute to OA pathogenesis both by directly amplifying ECM degradation and by exacerbating systemic metabolic inflammation via LPS production.

Several limitations should be considered when interpreting the present findings. First, this was an exploratory study with a relatively small sample size, especially in the two non-OA subgroups ($OB^+OA^-$ group (n=5) and the $OB^-OA^-$ group (n=7)), which may limit statistical power and generalisability. Given that the majority of our participants are senior, we were unable to fully confirm the presence of sub-clinical or radiological OA in the non-OA control group. Moreover, some participants had

a history of antibiotic use, particularly in the $OB^+OA^+$ group. Although antibiotic exposure was adjusted with other covariables in the differential analysis, its potential influence cannot be completely excluded. In addition, given the characteristic of the participants included in this study, some medications such as non-steroidal anti-inflammatory drugs (NSAIDs), metformin, and proton pump inhibitors might be commonly used, and they may also influence the gut microbial community. Unfortunately, these data were not collected in the current study. Therefore, future studies with larger and more balanced cohorts, along with more comprehensive medication information, are warranted to validate these observations. In addition, although all participants were instructed to complete the questionnaires, only 90 out of 103 were retrieved, which may introduce recall or reporting bias. Second, proteomic data were only available for 35 participants, and we examined correlations between 17 taxa and more than 5,400 proteins, resulting in over 90,000 statistical tests. Given the high dimensionality of the data, applying stringent multiple testing corrections would have markedly reduced statistical power and increased the risk of false negatives. Instead, we applied a conservative threshold of $p<0.001$ to reduce false positives while still prioritising potentially meaningful associations. Nevertheless, the possibility of residual false-positive findings cannot be excluded. Last, microbiomic profiling was performed using 16S rRNA gene sequencing, which provided reliable genus-level taxonomic resolution but lacked accuracy at the species or strain level (52). Since microbial functions can vary substantially within genera, future studies employing shotgun metagenomic sequencing will be important to achieve higher taxonomic and functional resolution.

As an emerging and rapidly evolving field, dietary modification and probiotic supplementation have been investigated as potential therapeutic approaches for joint disorders including rheumatoid arthritis (53) and OA (54). However, obesity-related OA represents a specific phenotype with its own distinct microbiomic characteristics. Our findings may offer valuable insights for the design of future clinical trials involving microbiome-based interventions such as microbiota transfer therapy. In addition, the associations we observed between gut microbiota and dietary patterns may help inform future studies exploring targeted dietary modification strategies on OA treatment.

## Conclusion

In conclusion, this exploratory study identified a distinct gut microbial signature in obesity-related knee OA patients, characterised by reduced α- and β-diversity and specific changes in bacterial abundances. These microbial shifts were associated with circulating metabolites and proteins involved in inflammation, lipid metabolism, and joint tissue regulation, while functional predictions suggested enhanced bile acid biosynthesis, glycosaminoglycan degradation, and LPS biosynthesis in obesity-related knee OA. Although the exact mechanisms require further validation, our findings suggested that gut microbiome plays a key role in linking OB to OA through systemic metabolic and inflammatory pathways, highlighting it as a potential target for future therapies.

## Acknowledgements

We thank all the study participants who made the study possible. The microbiomic profiling was done at the Integrated Microbiome Resource (Dalhousie University, Halifax, Canada); The metabolic profiling was done at The Metabolomics Innovation Centre (TMIC); The proteomic profiling was done at McGill Genome Centre.

## References

1. COLLABORATORS GBDO: Global, regional, and national burden of osteoarthritis, 1990-2020 and projections to 2050: a systematic analysis for the Global Burden of Disease Study 2021. *Lancet Rheumatol* 2023; 5: e508-e522. https://doi.org/10.1016/s2665-9913(23)00163-7
2. PALAZZO C, NGUYEN C, LEFEVRE-COLAU MM, RANNOU F, POIRAUDEAU S: Risk factors and burden of osteoarthritis. *Ann Phys Rehabil Med* 2016; 59: 134-38. https://doi.org/10.1016/j.rehab.2016.01.006
3. REYES C, LEYLAND KM, PEAT G, COOPER C, ARDEN NK, PRIETO-ALHAMBRA D: Association between overweight and obesity and risk of clinically diagnosed knee, hip, and hand osteoarthritis: a population-based cohort study. *Arthritis Rheumatol* 2016; 68: 1869-75. https://doi.org/10.1002/art.39707
4. SILVERWOOD V, BLAGOJEVIC-BUCKNALL M, JINKS C, JORDAN JL, PROTHEROE J, JORDAN KP: Current evidence on risk factors for knee osteoarthritis in older adults: a systematic review and meta-analysis. *Osteoarthritis Cartilage* 2015; 23: 507-15. https://doi.org/10.1016/j.joca.2014.11.019
5. KAMPS A, RUNHAAR J, TRAJANOSKA K *et al*.: Bidirectional causal relationship between obesity and osteoarthritis: insights from a two-sample Mendelian randomization study. *Osteoarthr Cartil Open* 2025; 7: 100636. https://doi.org/10.1016/j.ocarto.2025.100636
6. GRIFFIN TM, HUEBNER JL, KRAUS VB, YAN Z, GUILAK F: Induction of osteoarthritis and metabolic inflammation by a very high-fat diet in mice: effects of short-term exercise. *Arthritis Rheum* 2012; 64: 443-53. https://doi.org/10.1002/art.33332
7. SCHADLER P, LOHBERGER B, THAUERER B *et al*.: The association of blood biomarkers and body mass index in knee osteoarthritis: a cross-sectional study. *Cartilage* 2022; 13. https://doi.org/10.1177/19476035211069251
8. RUNHAAR J, SANCHEZ C, TARALLA S, HENROTIN Y, BIERMA-ZEINSTRA SM: Fibulin-3 fragments are prognostic biomarkers of osteoarthritis incidence in overweight and obese women. *Osteoarthritis Cartilage* 2016; 24: 672-78. https://doi.org/10.1016/j.joca.2015.10.013
9. CIRULLI ET, GUO L, LEON SWISHER C *et al*.: Profound perturbation of the metabolome in obesity is associated with health Risk. *Cell Metab* 2019; 29: 488-500 e482. https://doi.org/10.1016/j.cmet.2018.09.022
10. HUANG J, PAN F, LIU M *et al*.: Acyl-alkyl-phosphatidylcholine C40:6 is potentially a causal biomarker for obesity-related knee osteoarthritis: data from four independent cohorts. *Arthritis Rheumatol* 2025 (under review).
11. HA CW, LAM YY, HOLMES AJ: Mechanistic links between gut microbial community dynamics, microbial functions and metabolic health. *World J Gastroenterol* 2014; 20: 16498-517. https://doi.org/10.3748/wjg.v20.i44.16498
12. GILAT R, YAZDI AA, WEISSMAN AC *et al*.: The gut microbiome and joint microbiome show alterations in patients with knee osteoarthritis versus controls: a systematic review. *Arthroscopy* 2025; 41:1226-38. https://doi.org/10.1016/j.arthro.2024.05.010
13. HAN J, MENG X, KONG H, LI X, CHEN P, ZHANG XA: Links between short-chain fatty acids and osteoarthritis from pathology to clinic via gut-joint axis. *Stem Cell Res Ther* 2025; 16: 251. https://doi.org/10.1186/s13287-025-04386-3
14. DEN BESTEN G, VAN EUNEN K, GROEN AK, VENEMA K, REIJNGOUD DJ, BAKKER BM: The role of short-chain fatty acids in the interplay between diet, gut microbiota, and host energy metabolism. *J Lipid Res* 2013; 54: 2325-40. https://doi.org/10.1194/jlr.R036012
15. SCHOTT EM, FARNSWORTH CW, GRIER A *et*

*al*.: Targeting the gut microbiome to treat the osteoarthritis of obesity. *JCI Insight* 2018; 3. https://doi.org/10.1172/jci.insight.95997
16. HUANG J, LIU M, FUREY A, RAHMAN P, ZHAI G: Gut microbiomics of sustained knee pain in patients with knee osteoarthritis. *J Rheumatol* 2024; 51: 1218-25. https://doi.org/10.3899/jrheum.2024-0361
17. ALTMAN R, ALARCON G, APPELROUTH D *et al*.: The American College of Rheumatology criteria for the classification and reporting of osteoarthritis of the hip. *Arthritis Rheum* 1991; 34: 505-14. https://doi.org/10.1002/art.1780340502
18. LIU M, ZHANG H, XIE Z *et al*.: Glutathione, polyamine, and lysophosphatidylcholine synthesis pathways are associated with circulating pro-inflammatory cytokines. *Metabolomics* 2022; 18: 76. https://doi.org/10.1007/s11306-022-01932-5
19. AMIR A, MCDONALD D, NAVAS-MOLINA JA *et al*.: Deblur rapidly resolves single-nucleotide community sequence patterns. *mSystems* 2017; 2. https://doi.org/10.1128/msystems.00191-16
20. DOUGLAS GM, MAFFEI VJ, ZANEVELD JR *et al*.: PICRUSt2 for prediction of metagenome functions. *Nat Biotechnol* 2020; 38: 685-88. https://doi.org/10.1038/s41587-020-0548-6
21. KANEHISA M, GOTO S: KEGG: kyoto encyclopedia of genes and genomes. *Nucleic Acids Res* 2000; 28: 27-30. https://doi.org/10.1093/nar/28.1.27
22. HARRIS MA, CLARK J, IRELAND A *et al*.: The Gene Ontology (GO) database and informatics resource. *Nucleic Acids Res* 2004; 32: D258-261. https://doi.org/10.1093/nar/gkh036
23. OKSANEN J SIMPSOM GL, BLANCHET FG *et al*.: vegan: Community Ecology Package. R package version 2.6-4, (2022).
24. KEMBEL SW, COWAN PD, HELMUS MR *et al*.: Picante: R tools for integrating phylogenies and ecology. *Bioinformatics* 2010; 26: 1463-64. https://doi.org/10.1093/bioinformatics/btq166
25. WICKHAM H: ggplot2: elegant graphics for data analysis, viii, pp.212. (Springer, New York, 2009).
26. MALLICK H, RAHNAVARD A, MCIVER LJ *et al*.: Multivariable association discovery in population-scale meta-omics studies. *PLoS Comput Biol* 2021; 17: e1009442. https://doi.org/10.1371/journal.pcbi.1009442
27. MCMURDIE PJ, HOLMES S: phyloseq: an R package for reproducible interactive analysis and graphics of microbiome census data. *PLoS One* 2013; 8: e61217. https://doi.org/10.1371/journal.pone.0061217
28. YANG C, MAI J, CAO X, BURBERRY A, COMINELLI F, ZHANG L: ggpicrust2: an R package for PICRUSt2 predicted functional profile analysis and visualization. *Bioinformatics* 2023; 39. https://doi.org/10.1093/bioinformatics/btad470
29. LIN Y, XU Z, YEOH YK *et al*.: Combing fecal microbial community data to identify consistent obesity-specific microbial signatures and shared metabolic pathways. *iScience* 2023; 26: 106476. https://doi.org/10.1016/j.isci.2023.106476
30. WANG X, WU Y, LIU Y *et al*.: Altered gut microbiome profile in patients with knee osteoarthritis. *Front Microbiol* 2023; 14: 1153424. https://doi.org/10.3389/fmicb.2023.1153424
31. LOESER RF, ARBEEVA L, KELLEY K *et al*.: Association of increased serum lipopolysaccharide, but not microbial dysbiosis, with obesity-related osteoarthritis. *Arthritis Rheumatol* 2022; 74: 227-36. https://doi.org/10.1002/art.41955
32. ZHU Y, CHEN B, ZHANG X *et al*.: Exploration of the muribaculaceae family in the gut microbiota: diversity, metabolism, and function. *Nutrients* 2024; 16. https://doi.org/10.3390/nu16162660
33. LIU S, XU H, LIU L *et al*.: Gut microbiome dysbiosis accelerates osteoarthritis progression by inducing IFP-SM inflammation in "double-hit" mice. *Arthritis Res Ther* 2025; 27: 137. https://doi.org/10.1186/s13075-025-03602-y
34. CHO KH, NA HS, JHUN J *et al*.: Lactobacillus (LA-1) and butyrate inhibit osteoarthritis by controlling autophagy and inflammatory cell death of chondrocytes. *Front Immunol* 2022; 13: 930511. https://doi.org/10.3389/fimmu.2022.930511
35. ZHUANG H, REN X, JIANG F, ZHOU P: Indole-3-propionic acid alleviates chondrocytes inflammation and osteoarthritis via the AhR/NF-kappaB axis. *Mol Med* 2023; 29: 17. https://doi.org/10.1186/s10020-023-00614-9
36. XIE J, LI LF, DAI TY *et al*.: Short-chain fatty acids produced by ruminococcaceae mediate alpha-linolenic acid promote intestinal stem cells proliferation. *Mol Nutr Food Res* 2022; 66: e2100408. https://doi.org/10.1002/mnfr.202100408
37. DAI A, HOFFMAN K, XU AA *et al*.: The association between caffeine intake and the colonic mucosa-associated gut microbiota in humans-a preliminary investigation. *Nutrients* 2023; 15. https://doi.org/10.3390/nu15071747
38. YANG J, WANG H, LIN X *et al*.: Gut microbiota dysbiosis induced by alcohol exposure in pubertal and adult mice. *mSystems* 2024; 9: e0136624. https://doi.org/10.1128/msystems.01366-24
39. GUILLAN-FRESCO M, FRANCO-TREPAT E, ALONSO-PEREZ A *et al*.: Caffeine, a risk factor for osteoarthritis and longitudinal bone growth inhibition. *J Clin Med* 2020; 9. https://doi.org/10.3390/jcm9041163
40. LIU T, XU C, DRIBAN JB, MCALINDON T, EATON CB, LU B: Excessive alcohol consumption and the risk of knee osteoarthritis: a prospective study from the Osteoarthritis Initiative. *Osteoarthritis Cartilage* 2022; 30: 697-701. https://doi.org/10.1016/j.joca.2022.01.011
41. FU J, LI G, LI X, SONG S, CHENG L, RUI B, JIANG L: Gut commensal Alistipes as a potential pathogenic factor in colorectal cancer. *Discov Oncol* 2024; 15: 473. https://doi.org/10.1007/s12672-024-01393-3
42. CHEN J, WANG A, WANG Q: Dysbiosis of the gut microbiome is a risk factor for osteoarthritis in older female adults: a case control study. *BMC Bioinformatics* 2021; 22: 299. https://doi.org/10.1186/s12859-021-04199-0
43. WANG Z, ZHU H, JIANG Q, ZHU YZ: The gut microbiome as non-invasive biomarkers for identifying overweight people at risk for osteoarthritis. *Microb Pathog* 2021; 157: 104976. https://doi.org/10.1016/j.micpath.2021.104976
44. WOTING A, PFEIFFER N, LOH G, KLAUS S, BLAUT M: Clostridium ramosum promotes high-fat diet-induced obesity in gnotobiotic mouse models. *mBio* 2014; 5: e01530-01514. https://doi.org/10.1128/mbio.01530-14
45. SUN K, LUO J, GUO J, YAO X, JING X, GUO F: The PI3K/AKT/mTOR signaling pathway in osteoarthritis: a narrative review. *Osteoarthritis Cartilage* 2020; 28: 400-409. https://doi.org/10.1016/j.joca.2020.02.027
46. LI H, XIE S, QI Y, LI H, ZHANG R, LIAN Y: TNF-alpha increases the expression of inflammatory factors in synovial fibroblasts by inhibiting the PI3K/AKT pathway in a rat model of monosodium iodoacetate-induced osteoarthritis. *Exp Ther Med* 2018; 16:4737-4744. https://doi.org/10.3892/etm.2018.6770
47. DIAKITE MT, DIAKITE B, KONE A *et al*.: Relationships between gut microbiota, red meat consumption and colorectal cancer. *J Carcinog Mutagen* 2022; 13. doi:
48. LABBE A, GANOPOLSKY JG, MARTONI CJ, PRAKASH S, JONES ML: Bacterial bile metabolising gene abundance in Crohn's, ulcerative colitis and type 2 diabetes metagenomes. *PLoS One* 2014; 9: e115175. https://doi.org/10.1371/journal.pone.0115175
49. CHIANG JY: Bile acid metabolism and signaling. *Compr Physiol* 2013; 3: 1191-212. https://doi.org/ 10.1002/cphy.c120023
50. BANSAL PN, JOSHI NS, ENTEZARI V, GRINSTAFF MW, SNYDER BD: Contrast enhanced computed tomography can predict the glycosaminoglycan content and biomechanical properties of articular cartilage. *Osteoarthritis Cartilage* 2010; 18: 184-91. https://doi.org/10.1016/j.joca.2009.09.003
51. HUANG Z, KRAUS VB: Does lipopolysaccharide-mediated inflammation have a role in OA? *Nat Rev Rheumatol* 2016; 12: 123-29. https://doi.org/10.1038/nrrheum.2015.158
52. MATCHADO MS, RUHLEMANN M, REITMEIER S *et al*.: On the limits of 16S rRNA gene-based metagenome prediction and functional profiling. *Microb Genom* 2024; 10. https://doi.org/10.1099/mgen.0.001203
53. ZHENG Z, LIU X, ZHANG Y, ZHANG H, CHEN S, ZHU J: Research trends and hotspots on gut microbiota in rheumatoid arthritis: a bibliometric analysis from 2004 to 2024. *Clin Exp Rheumatol* 2025 Jun 5. https://doi.org/10.55563/clinexprheumatol/3899sf
54. TIAN M, ZHU Y, LU S *et al*.: Clinical efficacy of probiotic supplementation in the treatment of knee osteoarthritis: a meta-analysis. *Front Microbiol* 2025; 16: 1526690. https://doi.org/10.3389/fmicb.2025.1526690